Eur. Phys. J. D **45**, 229–234 (2007)
DOI: 10.1140/epjd/e2007-00277-3

THE EUROPEAN PHYSICAL JOURNAL D

Coherent control of ballistic energy growth for a kicked Bose-Einstein condensate

M. Sadgrove[1,a], M. Horikoshi[2,b], T. Sekimura[2], and K. Nakagawa[1,2]

[1] CREST, Japan Science and Technology Agency, Kawaguchi, Saitama 332-0012, Japan
[2] Institue for Laser Science, The University of Electro Communications, Chofushi, Chofugaoka 1-5-1, Japan

Received 8 June 2007
Published online 28 September 2007 –

Abstract. We consider a Bose-Einstein condensate which is split into two momentum components and then "kicked" at the Talbot time by an optical standing wave. The mean energy growth is shown to be suppressed or enhanced depending on the quantum phase between the two momentum components. Experimental verification is provided and we discuss possible implications of our results for recently suggested applications of kicked atoms.

PACS. 05.60.Gg Quantum transport – 05.45.Mt Quantum chaos; semiclassical methods – 03.75.Nt Other Bose-Einstein condensation phenomena

1 Introduction

Interference is a fundamental effect in quantum mechanics. In particular, the possibility of interference for objects which are classically point particles is one of the chief well-springs of so-called "quantum weirdness", that is, the counter-intuitive differences between classical and quantum mechanics. Moreover, quantum interference, along with entanglement, also offers an extra resource absent in classical physics which may be employed to improve measurement sensitivity [1] or to gain speed-ups over classical information processing algorithms [2,3].

In this letter we consider the possibilities that such interference presents for the *coherent control* of energy growth in the system known as the Atom Optics Kicked Rotor [4]. This system consists of cold atoms which receive sharp momentum kicks from a far-detuned optical standing wave with wave number k. The possibility of taking advantage of quantum interference effects in this setting has arisen due to the introduction of Bose-Einstein condensates (BEC) in kicked atom experiments [5]. Gong and Brumer have predicted that preparing the rotor in an initial superposition of momentum eigenstates allows quantum coherent control of the ensemble mean energy in both chaotic regimes [6] and at quantum resonance [7]. Indeed, it has already been demonstrated experimentally, that an initial superposition of 0 and 1 momentum eigenstates (in the units of the optical standing wave momentum quanta $2\hbar k$) can lead to a ratchet effect [8,9]. However, this arrangement does not allow non-trivial control of the ballistic energy growth for the atoms.

Here we use a BEC in a different initial configuration to [8,9] in order to examine control of the ballistic energy growth rate. Our system is comprised of a BEC which is coherently split into two momentum components separated by $4\hbar k$. This initial state is then subjected to sharp momentum "kicks" from a periodically pulsed optical standing wave. The two initial momentum components in superposition evolve in principle as separate dynamical systems but because they have phase coherence, quantum interference occurs leading to changes in the overall dynamics. In particular the rate at which the mean energy of the system increases may be suppressed or enhanced compared with the standard case by adjusting the quantum phase between the two systems.

2 Theory

The Hamiltonian for an atom which experiences δ-kicks with period T, is given by [10]

$$\hat{H} = \frac{\hat{p}^2}{2} + K\cos(2k\hat{x})\sum_t \delta(t' - t\tau), \qquad (1)$$

where $\hat{p}$ and $\hat{x}$ are the atomic momentum and position operators respectively, k is the kicking strength parameter, t' is time, t is the kick counter and $\tau = 4\pi T/66.3 \times 10^{-6}$ is the scaled kicking time.

The one kick evolution operator for atoms subject to a standing wave pulse followed by a period of free evolution is [11] $\hat{U} = \exp(-\mathrm{i}K\cos(2k\hat{x}))\exp(-\mathrm{i}\tau\hat{p}^2/2)$. In this paper, we are interested in what happens when the

[a] e-mail: mark@ils.uec.ac.jp
[b] *Present address*: Errato, c/o Institute of Engineering Innovation, The University of Tokyo, 2-11-16, Yayoi, Bunkyo-ku, Tokyo 113-8656, Japan.

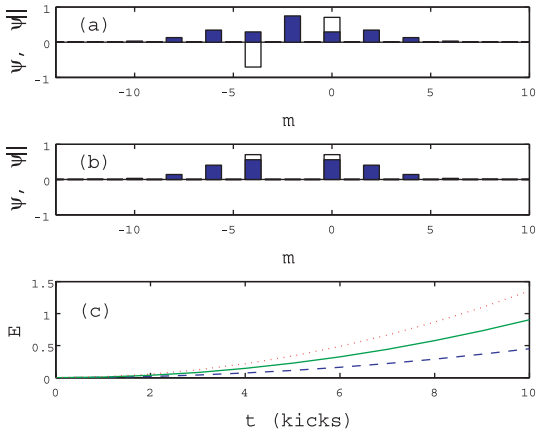

Fig. 1. (Color online) Theoretical wavefunctions ((a) and (b)) and energy vs. time curves for interfering kicked rotor systems with $k = 0.14$. In (a), the unfilled bars show the initial wavefunction for which the quantum phase is $\phi = \pi$. The filled bars show the absolute value of the wave function (i.e. the square root of the momentum distribution) after 7 kicks. In (b) the case for $\phi = 0$ is shown for the same parameters. In (c) the mean energy of the atomic ensemble is shown (minus the initial energy) for $\phi = \pi$ (dashed line), $\phi = 0$ (dotted line) and the standard result (i.e. where there is only one kicked rotor system and no quantum interference) (solid line).

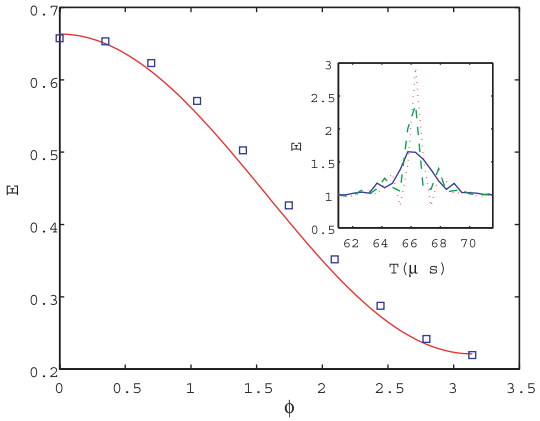

Fig. 2. (Color online) The mean energy of a kicked superposition state after 7 kicks as a function of the quantum phase ϕ for $k = 0.14$. The solid line shows the theory given in equation (5), and the squares show data from quantum simulations. Crosses show experimental data for three values of ϕ and the circle marks the value measured in the case of no initial Bragg diffraction (which was used to determine k for these experiments). The inset shows simulation energies as a function of the kicking period T demonstrating the suppressed height of the quantum resonance peak for the $\phi = \pi$ case (solid line) compared with the $\phi = \pi/2$ case (dashed line) and the enhancement which is possible in the $\phi = \pi$ case (dotted line).

quantum resonance condition is fulfilled, namely that the atoms start in an initial momentum eigenstate (or superposition thereof) and that the pulse period is equal to the Talbot time (or $\tau = 4\pi$). In this case, it may be shown that the second exponential term reduces to unity and the evolution operator for quantum resonance becomes $\hat{U}_{\mathrm{q.r.}}(t) = \exp(-\mathrm{i}Kt\cos(2k\hat{x}))$.

We now extend the analytical results of reference [11] to the case where the initial state is of the form

$$|\psi_{\mathrm{i}}\rangle = 1/\sqrt{2}(|0\hbar k\rangle - \mathrm{e}^{\mathrm{i}\phi}|-4\hbar k\rangle) \equiv 1/\sqrt{2}(|0\rangle - \mathrm{e}^{\mathrm{i}\phi}|-2\rangle), \tag{2}$$

where the superposed states are momentum eigenstates defined by $\hat{p}|n\rangle = n|n\rangle$. Cohen's result [12] $\psi_o(m) = \langle m|\hat{U}_{\mathrm{q.r.}}|n\rangle = (-i)^{m-n}J_{m-n}(Kt)$ may be used to find the output wavefunction ψ_o after kicking and thus the theoretical momentum distribution $P(m) = |\psi_o|^2$, giving

$$P(m) = \frac{1}{2}J_m^2(Kt) + \frac{1}{2}J_{m+2}^2(Kt) + \cos\phi J_m(Kt)J_{m+2}(Kt). \tag{3}$$

The first two terms in this equation are the usual momentum distributions for atoms starting with momenta 0 and $-4\hbar k$ respectively and kicked at quantum resonance [11]. The final term is an interference term which modifies the overall momentum distribution. Predicted wavefunctions for the cases where $\phi = \pi$ and $\phi = 0$ are shown in Figures 1a and 1b respectively. For the $\phi = \pi$ case, the momentum spread of the atoms is suppressed due to constructive interference of atoms in the $-2\hbar k$ momentum state and corresponding destructive interference at higher momenta. Conversely when the phase is set to 0, destructive interference in the $-2\hbar k$ momentum state leads to redistribution of atoms to higher momenta and a consequent increase in the mean energy. The mean energy may be calculated by evaluating the second moment of the momentum distribution $2E = \langle p^2\rangle = \sum_m m^2 P_n(m)$. Substituting 3 gives

$$\begin{aligned} E(k,t) &= \frac{1}{4}K^2t^2 + \cos\phi\sum_m m^2 J_m(Kt)J_{m+2}(Kt) \\ &= \frac{1}{4}K^2t^2 + \cos\phi C(Kt), \end{aligned} \tag{4}$$

where $C(Kt) = \sum_m m^2 J_m(Kt)J_{m+2}(Kt)$. $C_n(z)$ may be evaluated by successive applications of the Bessel recursion formula $mJ_m(z) = z/2(J_{m-1}(z) + J_{m+1}(z))$ along with Graf's theorem [13] giving $C_n(z) = z^2/4$. Thus the mean energy of the interfering kicked rotor system is given by

$$E(Kt) = \frac{1}{4}K^2t^2 + \cos(\phi)\frac{1}{8}K^2t^2. \tag{5}$$

Equation (5) shows that in principle, the energy growth rate at quantum resonance *can be suppressed or enhanced* by up to 50% by varying the relative phase between the two momentum states as shown in Figure 2. This *coherent control* of the dynamics is afforded by quantum interference which redistributes atoms into higher or lower momentum orders depending on the quantum phase. The inset to Figure 2 shows simulated energies as the kicking period T is swept over the quantum resonance at $T = T_T$ for three different values of the quantum phase ϕ. It may be seen that the interference effect gives rise to broadening and narrowing of the peak for $\phi = \pi$ and $\phi = 0$

respectively. Figure 2 also shows quantum simulation results for comparison with the theory. The simulations are of the single particle Hamiltonian (1), since on the time scales of the experiments performed here, atom-atom interactions in the BEC and also the effect of the harmonic trap potential may be ignored [5]. We note from the outset that the increase in the energy growth rate found here *cannot* be gained just by redefining the time at which the first kick occurs in the normal kicked rotor. For example, defining the first j kicks as a state preparation phase gives $E = (1/4)K^2(t+j)^2$, i.e. the energy increases faster than the usual case due to redefinition of the time origin. However the coefficient of ballistic growth *cannot* be changed by a mere shifting of the time origin in the standard kicked rotor experiment. It turns out that for the rectified diffusion experiment performed previously [8], any increase in the energy growth rate due to the initial superposition is merely of this trivial kind. The effect seen in this paper is new precisely because it leads to a non-trivial increase in the ballistic growth coefficient itself (conversely, no ratchet effect is observed for the configuration considered here).

It is also worth noting that, until now, the maximum energy growth rate for kicked atoms was $k^2t/2$, which generally occurs for atoms in an initial momentum eigenstate kicked at quantum resonance[1]. However, this growth rate is also found in the *semiclassical* limit of the kicked rotor, as shown in reference [18]. Therefore, it is fair to say that until now, the quantum kicked rotor has not been able to *exceed* the classical maximum momentum diffusion rate. The effect seen here, however, uses quantum coherence to push the diffusion rate above the classical maximum.

3 Experimental results

We now consider the experimental verification of equation (3). In order to realise the system experimentally, we use a combination of Bragg diffraction of atoms to create the initial superposition state required, followed by the usual kicking procedure used to realise the atom optics kicked rotor (AOKR) with atoms in a pulsed standing wave [4]. Our basic experimental setup and method has been explained in detail elsewhere [14,15]. The main details are as follows: A BEC of $\sim 3 \times 10^3$ ^{87}Rb atoms is realised and loaded onto an atom chip [15]. The atoms are trapped in the $5S_{1/2}$, $F = 2$, $m_f = 2$ state by the magnetic field generated by the chip and sit 700 μm below the chip surface. Typically, the axial trapping frequency for the BEC is $\omega_z \approx 2\pi \times 17$ Hz and the axial and radial Thomas-Fermi radii are $d_z = 17$ μm and $d_\rho = 3$ μm respectively.

As discussed in reference [8] our experiments consist of an initial state engineering phase, to prepare the BEC in a desired momentum superposition state, followed by a kicking phase to induce the resonant transport of the atoms. This is followed by standard absorption imaging of the BEC after a 25 ms flight time [14].

Experimentally, preparation of the initial state is achieved through the combination of a Bragg pulse followed by a period Δ_ϕ of free evolution to adjust the quantum phase. Two counterpropagating beams are aligned along the z-axis of the condensate to provide the Bragg/kicking beams for the experiment. The beams have a Gaussian profile with a half width of $\sim$1.0 mm. The optical power is 5 mW and the detuning from the ^{87}Rb $5^2S_{1/2} \rightarrow 5^2P_{3/2}$ resonance is $\sim$4 GHz. We use the same two beams to provide both the Bragg pulse and the kicking pulses. However the parameters required in each case are quite different. To solve this problem we use two synchronised Agilent 33250A function generators to provide driving signals for the AOMs which control each Bragg beam. We control the frequency of one generator using frequency shift keyed (FSK) modulation to provide the required frequency difference $\Delta\omega$ between the two Bragg beams, and use externally gated amplitude modulation of the other generator to ensure that the geometric mean $\sqrt{I_1 I_2}$ of the Bragg beams is sufficiently low to give coherent Bragg diffraction over a pulse interval of $\Delta_B \sim 100$ μs (for a $\pi/2$ pulse). In the experiments described here, the amplitude of beam 1 is reduced to $I_B = 0.12 I_0$ for the Bragg pulse. The envelope of the pulses, (including the quantum phase accumulation time and kicking) Δ_ϕ and the timing of the FSK and amplitude modulation is controlled by an additional function generator (NF Wavefactory 1966).

Because the BEC is so cold ($\approx$10 nK) it may be considered, to a good approximation, to be in a $|0\hbar k\rangle$ momentum eigenstate before the state engineering phase [14]. This assertion is supported by the recent measurements of high order quantum resonances made using a BEC as reported recently by Ryu et al. [16]. In that study, ballistic momentum growth was observed for up to 20 kicks — almost three times as many as studied here — and no significant variation was observed due to the small non-zero quasimomentum of the atoms[2]. If we choose $\Delta\omega = 8\omega_r$ where (where $\omega_r \approx 2.37 \times 10^4$ Hz is the recoil frequency of ^{87}Rb) the state after application of the Bragg $\pi/2$ pulse is given by

$$|\psi_i\rangle = \frac{1}{\sqrt{2}}|0\hbar k\rangle - \frac{1}{\sqrt{2}}|-4\hbar k\rangle. \tag{6}$$

The atoms are then allowed to evolve freely for a time Δ_ϕ giving rise to a relative phase shift between the superposed states of $\phi = (8\hbar k_l^2)t/M_{\mathrm{Rb}} \approx 9.48 \times 10^4 \Delta_\phi$, and the state just before kicking occurs is then

$$|\psi_i\rangle = \frac{1}{\sqrt{2}}(|0\hbar k\rangle - \mathrm{e}^{\mathrm{i}\phi}|-4\hbar k\rangle), \tag{7}$$

as assumed by the theory in equation (2). After the initial preparation of the atomic wavefunction, the frequency and intensity of the beams is made equal to provide the optical standing wave necessary for kicking. As in other

[1] Away from quantum resonance, the growth rate oscillates about the quasilinear value $k^2/4$ before dynamical localisation sets in.

[2] In line with the predictions of reference [20], however, it would be expected that after a large number of kicks, the non-zero momentum width of the condensate would result in sub-ballistic energy growth.

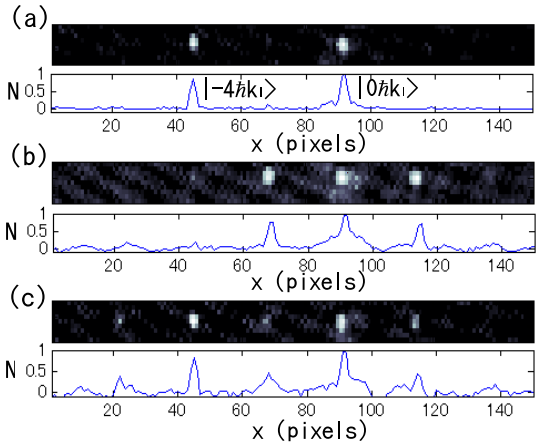

Fig. 3. Images of initial state preparation and kicking of the BEC with corresponding image cross sections showing the relative atomic population N. (a) shows the BEC after preparation of an approximate $|\psi_i\rangle = (1/\sqrt{2})(|0\hbar k\rangle + |-4\hbar k\rangle)$ initial state using a Bragg $\pi/2$ pulse. The $|0\hbar k\rangle$ and $|-4\hbar k\rangle$ are indicated. In (b) atoms were diffracted by 3 kicks starting from an initial $|0\hbar k\rangle$ eigenstate, whereas in (c) the kicks were applied after the preparation of the BEC in state ψ_i. The noise floor has been suppressed in the images only, allowing a clearer picture of the atoms. The cross sections were created by summing over the rows of the images.

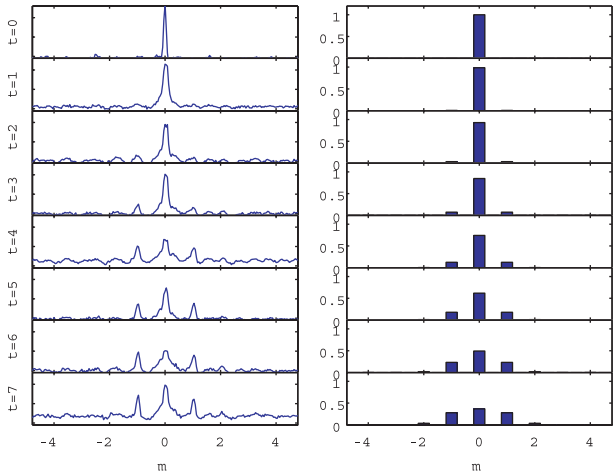

Fig. 4. Experimental (left column) and theoretical (right column) atomic momentum distributions are shown for the case of no initial superposition state. The vertical axis of the experimental data is in arbitrary units, whilst the horizontal axis shows the momentum m in units of $2\hbar k$. The simulations are for $k = 0.14$. Atoms are coupled symmetrically into higher momentum orders about the 0 momentum eigenstate.

recent reports, we have found that performing the kicking experiments *in trap* is not problematic since the energy gained by the atoms due to kicking far exceeds the trapping frequency and atom-atom interactions [5]. Therefore a single particle analysis is sufficient to describe the dynamics as we now show. For the analytical solution of the atomic dynamics, we assumed that the kicking pulses were ideal δ functions. Although this is not well approximated in most experiments, the analytical predictions turn out to be remarkably robust against non-zero pulse widths and non-rectangular pulse shapes so long as the number of kicks and mean atomic energy remains low [17,18].

In our experiments, the atoms are imaged after kicking using standard absorption imaging techniques [14]. The resulting atomic distribution can then be analysed to calculate the atomic momentum distribution and also the mean energy of the kicked atomic ensemble. Figure 3a shows an absorption image of the BEC after application of a Bragg $\pi/2$ pulse with $\Delta\omega \approx 30$ kHz and with no kicking applied. The atoms are clearly separated into two distinct momentum classes of roughly equal amplitude. The lower plot of Figure 3a shows a 1D atomic density distribution calculated by summing over the rows of the absorption image. Because the momentum separation of each group of diffracted atoms is known to be $2\hbar k$, the final momentum distribution of the atoms may be inferred from the normalised density distribution. In Figure 3b a kicked condensate is shown (starting from an initial $|0\hbar k\rangle$ eigenstate) after 3 kicks have been delivered demonstrating the usual diffraction of atoms into higher momentum orders. In Figure 3c the same thing is shown for a condensate which has been prepared in the initial state $|\psi_i\rangle$. We note that as more kicks are delivered, the signal-to-noise ratio of the data becomes noticeably worse as the condensate is diffracted into higher momentum orders, which prevents us from probing high kick numbers or kicking strengths for these experiments.

Figures 4–6 show experimentally obtained momentum distributions after 7 kicks for the experimental realisation of the interfering kicked rotor system alongside theoretically predicted momentum distributions. Figure 4 shows the "control" case in which the initial state is $|0\hbar k\rangle$. From the observed diffraction, the kick strength parameter k was estimated to be 0.14 and this value has been used to create the theoretical distributions shown in the right hand column. In Figure 5 the initial state was prepared in the superposition state $|\psi_i\rangle$ with a relative quantum phase $\phi = \pi$ between the states. As can be seen this leads to a marked increase in the number of atoms in the central momentum state (which is $|-2\hbar k\rangle$) leading to a lower momentum spread and hence mean energy than that found in the control case.

For $\phi = 0$, as seen in Figure 6, the momentum spread about $-2\hbar k$ is greatly enhanced compared with the $\phi = \pi$ case. Most notably, the population of the $-2\hbar k$ state remains relatively small compared with the other states for the first few kicks, unlike the case for $\phi = \pi$. We note however, that although this larger momentum spread is in qualitative agreement with equation (3) the observed momentum distributions do not agree so well quantitatively with the theoretical predictions. In fact, although we were able to show suppression of energy growth consistently in our experiments, enhancement of the energy growth coefficient was not clearly observed in all cases. The enhancement effect relies on the precise cancellation of the atomic momentum-space wavefunction at $-2\hbar k$, which can easily be ruined by slight fluctuations in the

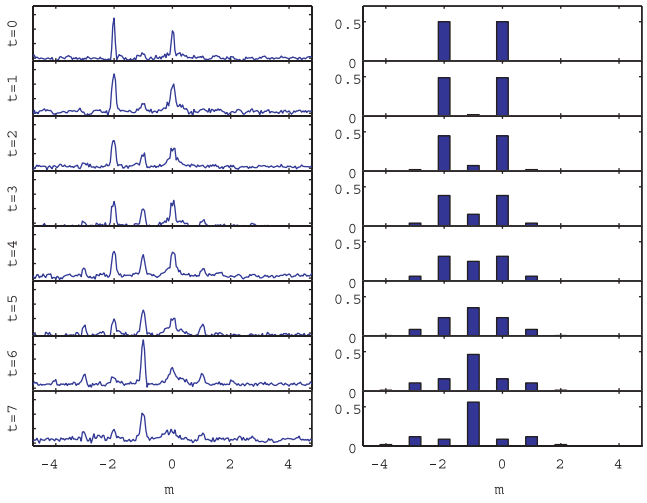

Fig. 5. Experimental (left column) and theoretical (right column) atom distributions are shown for the case an initial superposition state with $\phi = \pi$. The simulations are for $k = 0.14$. Suppression of momentum growth by constructive interference in the $-\hbar k$ momentum state is clearly seen.

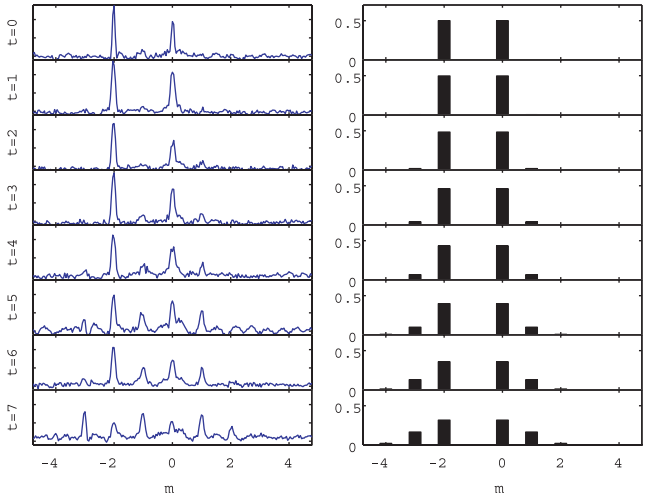

Fig. 6. Same as Figure 5 but with $\phi = 0$.

power and detuning of the free running Bragg laser which lead to slight inequalities in the populations of the $0\hbar k$ and $-4\hbar k$ states or even slight population of the $-2\hbar k$ momentum order in the initial state. Indeed, some asymmetry is apparent in the initial superposition state. Such experimental imperfections ruin the interference required to reliably demonstrate the enhancement effect in the lab. This situation could be improved by introducing a separate laser for performing Bragg diffraction which could be further detuned from atomic resonance, thus reducing the effect of small fluctuations in wavelength or power of the laser. Nonetheless, the experimental results demonstrate that the interference effect occurs and leads to the alteration of the energy growth rate compared with the standard result. In the current experiments, it proved difficult to accurately measure the mean energy from the atomic momentum distribution mainly due to the low atom number and the resulting low signal to noise ratio. Future experiments with increased atom number should enable the reliable measurement of the theoretical curves seen in Figure 2.

4 Discussion

It seems pertinent to ask whether any other easily preparable momentum states offer the same benefits as the $|\psi\rangle = (1/\sqrt{2})(|0\hbar k\rangle - |-4\hbar k\rangle)$ state. After all, in a standard kicked rotor experiment, starting from a single momentum eigenstate, the first kick creates a momentum superposition state whose components then interfere during subsequent kicks. However, although the standard kicked rotor experiments essentially involve a kicked superposition state after the first kick, there is no way to control the quantum phase or amplitude of each momentum state in the superposition. Engineering the initial state to have a specific relative quantum phase and amplitude is the feature that allows the ballistic diffusion rate to be controlled in this investigation. It has been shown that a superposition of the $0\hbar k$ and $-2\hbar k$ eigenstates leads to directional momentum transport [8,9], although, as noted earlier, no control over the ballistic growth rate is available in this case. Furthermore, numerical simulations suggest that initial superpositions of two states separated by more than $4\hbar k$ in momentum space do not exhibit quantum phase dependent changes in the diffusion rate.

We now speculate as to the possible advantages of the system studied here in applications compared with the normal kicked atom system. In the first place we consider the utility of the standard quantum resonance effect as augmented by our technique. As first shown in reference [19] for the two frequency kicked rotor system, the kicked rotor system contains resonances which exhibit sub-Fourier narrowing with time, potentially allowing the differentiation of two frequencies in a time which beats the Fourier limit. This feature is due to the nonlinear nature of the quantum kicked rotor. The quantum resonance in mean energy employed in this paper has also been shown to exhibit such sub-Fourier scaling of the resonance width with time (a property which can be explained using a semi-classical description of the quantum resonance) [20]. Therefore, one could in principle distinguish the difference between a kicking signal's frequency and exact quantum resonant frequency in sub-Fourier time by monitoring the width of the atomic momentum distribution of the kicked atoms. Our method can *increase* the sharpness of the quantum resonance curve (see the inset of Fig. 2) thereby providing a purely quantum increase to the sensitivity of any sub-Fourier frequency measurement schemes (although it should be noted that the overall scaling of the resonance peaks is expected to remain the same).

More generally, the increase in energy diffusion over the classical value may give rise to a quantum-over-classical speed-up in any process which relies on momentum diffusion. To use a contemporary example, recent

studies suggest links between quantum resonance and discrete time *quantum random walks* (QRW) [21]. QRW are of interest partially because they can be used to implement quantum search algorithms [22]. Very recently, there has been a proposal to implement QRW using a BEC in a momentum superposition state such as that used here [24]. Additionally, there is a separate proposal for implementing QRW in kicked cold atoms using a superposition of internal atomic electronic states to create the "quantum coin" effect needed for QRW [23]. Because the quantum random walk takes place in momentum space, it may be possible to use an additional superposition of momentum states to enhance the momentum diffusion, hence speeding up the random walk through momentum space and plausibly any algorithm based on the random walk.

Lastly, we note the possibility of using the effect seen here is to distinguish the phase of momentum eigenstates in a superposition. In principle, for superpositions of several different eigenstates, the interference properties we have explored for a two state superposition should uniquely identify a single phase flipped state amongst a superposition otherwise consisting of states with 0 relative phase, since the output momentum distribution depends sensitively on interference between the states in superposition (a similar effect has also been noted by Gong [7]). Assuming that it is possible to set the phase of each eigenstate independently, this suggests the possibility of storage and retrieval of information using the quantum phase of the eigenstates in a similar way to that performed with Rydberg atoms in reference [25] (which are also promising due to the existence of stable quantum wave packets for Rydberg atoms [26]). That is, starting from an initial superposition state, the operations afforded by applying pulses from an optical lattice are conceivably sufficient to perform some quantum information processing algorithms on the states in superposition (although such a scheme would certainly not be a universal quantum computer). This idea is the subject of ongoing research.

In conclusion, we have presented a method of coherently controlling the ballistic quantum transport of atoms subject to Talbot pulses from an optical lattice. The method uses quantum interference between two coherent kicked atom systems to adjust the ballistic growth rate of the kicked atoms by up to 50%. The observed effect may be explained in terms of the interference between the matterwaves diffracted from the two initial sources. We expect that recent proposals for making use of the properties of quantum resonant dynamics will benefit from similar quantum interference methods.

This work was partly supported by a Grant-in-Aids for Science Research (17340120) from the Ministry of Education, Science, Sports and Culture, and the 21st Century COE program on "Coherent Optical Science".

References

1. M.R. Andrews et al., Science **275**, 637 (1997); M. Kozuma et al., Science **286**, 2309 (1999); M.A. Kasevich, Science **298**, 1363 (2002); Y. Wang et al., Phys. Rev. Lett. **94**, 090405 (2005)
2. L.K. Grover, Phys. Rev. Lett. **79**, 325 (1997)
3. S. Loyd, Phys. Rev. A **61**, 010301(R) (1999)
4. F.L. Moore et al., Phys. Rev. Lett. **75**, 4598 (1995)
5. G.J. Duffy et al., Phys. Rev. A **70**, 041602(R) (2004); S. Wimberger et al., Phys. Rev. Lett. **94**, 130404 (2005); G. Behinaein et al., Phys. Rev. Lett. **97**, 244101 (2006)
6. J. Gong, P. Brumer, Phys. Rev. Lett. **86**, 1741 (2001)
7. J. Gong, personal communication
8. M. Sadgrove, Horikoshi Munekazu, Tetsuo Sekimura, Ken'ichi Nakagawa, Phys. Rev. Lett. **99**, 043002 (2007)
9. I. Dana, V. Ramareddy, I. Talukdar, G.S. Summy, e-print `arXiv:0706.0871v1 [physics.atom-ph]`
10. R. Graham, M. Schlautmann, P. Zoller, Phys. Rev. A **45**, 19(R) (1992)
11. F.M. Izrailev, D.L. Shepelyanskii, Dokl. Akad. Nauk SSSR **256**, 586 (1981)
12. D. Cohen, Phys. Rev. A **44**, 2292 (1991)
13. G.N. Watson, *A treatise on the theory of Bessel functions* (Cambridge Univ. Press, 1996)
14. M. Horikoshi, K. Nakagawa, Phys. Rev. A **74**, 031602(R) (2006)
15. M. Horikoshi, K. Nakagawa, Appl. Phys. B **82**, 363 (2006)
16. C. Ryu et al., Phys. Rev. Lett. **96**, 160403 (2006)
17. R. Blümel, S. Fishman, U. Smilansky, J. Chem. Phys. **84**, 2604 (1986)
18. M. Sadgrove et al., Phys. Rev. Lett. **94**, 174103 (2005)
19. P. Szriftgiser et al., Phys. Rev. Lett. **89**, 224101 (2002)
20. S. Wimberger, I. Guarneri, S. Fishman, Nonlin. **16**, 1381 (2003)
21. O. Buerschaper, K. Burnett, e-print `quant-ph/0406039`
22. N. Shenvi, J. Kempe, K. Birgitta Whaley, Phys. Rev. A **67**, 052307 (2003)
23. Z.-Y. Ma et al., Phys. Rev. A **73**, 013401 (2006)
24. C.M. Chandrashekar, e-print `quant-ph/0603156v4`
25. J. Ahn, T.C. Weinacht, P.H. Bucksbaum, Science **287**, 463 (2000)
26. A. Buchleitner, D. Delande, J. Zakrewski, Phys. Rep. **368**, 409 (2002)